A Distributionally Robust Chance-Constrained Power Line De-energization Method for Wildfire Mitigation

Fasiha Zainab
Department of Electrical and Computer Engineering
Mississippi State University
Starkville, MS, USA
fz94@msstate.edu

Yong Fu
Department of Electrical and Computer Engineering
Mississippi State University
Starkville, MS, USA
fu@ece.msstate.edu

***Abstract*— The growing occurrence of power system–induced wildfires have become a major threat to the reliable operation of power systems. To address this issue, this paper introduces a model that considers uncertain weather conditions (e.g., wind speed) to estimate the wildfire risk of power lines. In order to capture the uncertainty associated with weather conditions, a Wasserstein distance–based ambiguity set is employed. To this end, a distributionally robust chance-constrained line de-energization model (DRCC-LDM) is proposed, in which the wildfire risk mitigation constraint is formulated as a chance constraint. The proposed model determines de-energization decisions of power lines to effectively mitigate wildfire risk while minimizing load shedding, which is solved using a mixed-integer second-order conic programming (MISOCP) method. Case studies on the RTS-GMLC 73-bus system demonstrate the effectiveness of the proposed DRCC-LDM in mitigating wildfire risk.**

Keywords—Distributionally robust chance-constrained, load shedding, power system resilience, and wildfire risk.

I. INTRODUCTION

In recent years, the frequency and severity of natural disaster events have become more frequent and severe, posing significant threats to public safety and infrastructure. For instance, the United States experienced more than fifty thousand wildfire-related events in 2020, causing serious damage to infrastructure and power systems [1].

Wildfire and power systems have two-way interaction, whereas the power system can be affected by the wildfires initiated by natural phenomena such as lightning and high temperatures, while power systems can also serve as a potential source of wildfire ignition. Power systems-induced wildfires occur in multiple ways, while the most common ways are the direct contact of vegetation with conductors due to high wind speed and faulty power lines [2]. Due to the malfunction of the power line, the most destructive 2018 Camp Fire in California sparked when the transmission line encountered vegetation due to strong katabatic winds. This fire affected more than 50,000 people and damaged over 18,000 infrastructures [3]. One of the two fires in Texas began when winds knocked a tree onto power lines, while the other fire was started due to fallen tree branches tangled with power lines, exposing communities and infrastructure to damage and service interruptions [4]. From 2016 to 2020, the number of power system-induced wildfires increased by approximately 19%, as indicated by [5]. To reduce the likelihood of wildfire ignition, preventive measures involve timely vegetation management, proper inspection and maintenance of electrical equipment [6]. However, from the short-term perspective, preventive measures require critical decision-making strategies by utility operators to prevent wildfire events. To mitigate the growing wildfire risk, PG&E in 2018 implemented its intentional blackout program known as public safety power shutoff (PSPS) [7]. A decision-making approach for wildfire risk mitigation is developed in [8], which finds a trade-off between wildfire risk and power delivery, aiming to maximize the amount of power supplied to the load while minimizing the wildfire risk. Moreover, the security-constrained optimal power shutoff method is proposed in [9], which finds a tradeoff between both wildfire risk and pre-and post-contingency load shedding. However, these methods do not account for uncertain weather conditions in the wildfire risk estimation. A multi-period study [10] implements a proactive stochastic programming (SP) framework that models wildfire scenarios as either endogenous or exogenous fire events to maximize load delivery and minimize the wildfire impact. As the wildfire risk is uncertain, the study in [11] considers scenarios where the wildfire risk is known with low and high confidence that jointly minimize generation and load-shedding costs in the face of uncertain fire risk. The author in [12] employs a stochastic wildfire simulation approach to generate wildfire scenarios, which are then incorporated into a robust optimization (RO) framework to identify worst-case contingencies induced by the wildfires.

To estimate the wildfire risk arising from uncertain weather conditions, most studies employ SP and RO techniques, where SP relies heavily on the predetermined probability distributions of uncertainties, while RO does not incorporate any probabilistic information of the uncertainties. Considering the limitations of both SP and RO methods, distributionally robust chance-constrained (DRCC) optimization accounts for a family of probability distributions when only partial knowledge of the probability distribution is available [13]. Rather than relying on an accurate underlying distribution, DRCC defines an ambiguity set, which captures a range of plausible distributions. This ambiguity set can be constructed using various approaches, such as moment-based or distance-based methods.

To address the above-mentioned challenges, this study proposed a model in which the probability of ignition of the power line is explicitly estimated by accounting for uncertain weather conditions (e.g., uncertainties arising from wind speed conditions). To capture these uncertainties, the wildfire risk mitigation constraint is formulated as a chance constraint over a Wasserstein distance-based ambiguity set, chosen for its better out-of-sample performance. This paper presents a distributionally robust chance-constrained power line de-energization method (DRCC-LDM) where the model optimally de-energizes lines to mitigate wildfire risks, while the objective

979-8-3315-8138-1

minimizes the resulting load shedding cost. This approach is adopted to effectively enhance the resilience of the power system under uncertain weather conditions.

The remainder of the paper is organized as follows. Section II introduces the proposed DRCC-LDM. Section III discusses the solution methodology of the DRCC-LDM. Case studies are presented in Section IV. Conclusions are drawn in Section V.

II. Proposed DRCC-LDM Model

This section explains the estimation of wildfire risk, the generic formulation of DRCC, the construction of the ambiguity set, and the mathematical formulation of our proposed DRCC-LDM model.

A. Estimation of Wildfire Risk

In our study, wildfire risk is represented as a risk triangle consisting of the three elements, as shown below,

$$r_{jk}^{f} = \rho_{jk}^{f} \times I_{jk} \times E_{jk} \tag{1}$$

Here, r_{jk}^{f} represents the wildfire risk associated with the transmission line jk and the ρ_{jk}^{f} denotes the probability of ignition. In this study, the probability of ignition corresponds to the probability that a fault in the transmission line causes ignition. Moreover, I_{jk} and E_{jk} represents the intensity and effect of a fire, where intensity describes the strength at which fire initiates, such as low, medium, and high (e.g. $I_{jk} = 1, 2, 3,$ respectively), while the effect is the damage of fire to the highly valued resources expressed as the percentage loss of highly valued resources (e.g. 100%). From the perspective of power system-induced wildfire, the fire intensity and effect can only be estimated once the fire is initiated, while utilities can only control the probability of ignition due to a fault in transmission line that causes fire. The probability of ignition, where a fault in the transmission line initiates fire, depends on the line characteristics such as fault condition, maintenance status, age of line, recent vegetation management along the line, as well as uncertain wind speed conditions. For example, higher wind speed increases the chances of interaction between power lines and nearby vegetation, thereby raising the probability of igniting a fire. In order to find a relationship between line characteristics and uncertain wind speed, a Poisson regression model is implemented [14], which helps to estimate the probability of ignition. To account the spatial and temporal variations in the dataset, the data is divided into multiple areas and periods. The sorted data is then used to estimate the Poisson model parameter, which represents the ignition rate $\hat{\lambda}$ defined as the number of ignition occurrences per unit time and length. The regression model is employed to establish a relationship between the ignition rate $\hat{\lambda}$, line characteristics, and uncertain wind speed, which can be expressed as follows,

$$\bar{\lambda} = ln(\hat{\lambda}) = b_0 + b_1 w \tag{2}$$

where, $\bar{\lambda}$ is defined to denote the logarithm of $\hat{\lambda}$; $b = (b_0, b_1)$ is the regression coefficient vector; and w represents wind speed. Here, b_0 captures the ignition rate due to line characteristics. The term $b_1 w_1$ estimate the ignition rate due to uncertain wind speed w. The probability of ignition in each line area can be determined by using $\bar{\lambda}$. In this model, each transmission line corresponds to a specific area, allowing the probability of ignition of a transmission line to be calculated as,

$$\rho_{jk}^{f} = 1 - e^{-\bar{\lambda}_{jk}} \tag{3}$$

B. Generic Formulation of DRCC

In order to handle uncertainties, a typical chance-constrained (CC) problem is generalized by (4),

$$\min_{x \in X} \; c^T x$$
$$\text{s.t. } \mathbb{P}_u \left(A(\tilde{\xi}) x \geq b(\tilde{\xi}) \right) \geq 1 - \epsilon \tag{4}$$

where x and c represent the decision variable and its cost coefficient vector, respectively. The feasible region is X. The random vector $\tilde{\xi}$ follows the probability distribution $\mathbb{P}_u$. Also, $A(\tilde{\xi})$ represents a technology matrix of random constraint coefficients, $b(\tilde{\xi})$ denotes a vector of random right-hand side (RHS), and ϵ is the risk tolerance. The probability of violating the constraint $A(\tilde{\xi})x \geq b(\tilde{\xi})$ is no more than ϵ, which allows the model to satisfy a certain confidence level $(1 - \epsilon)$ at least.

Note that it can be challenging to obtain the exact $\mathbb{P}_u$ information about the uncertainty when the underlying distribution $\mathbb{P}_u$ is ambiguous. Therefore, the solution of the CC model (4) can be highly dependent on the choice of P_u. Rather than assuming a specific distribution of uncertainty, a preferable way is to implement a set of plausible probability distributions when the true distribution of the random parameters $\tilde{\xi}$ is ambiguous. We suppose that the $\mathbb{P}_u$ of $\tilde{\xi}$ lies within an ambiguity set U , encompassing all plausible distributions. Thus, the DRCC model is defined as follows,

$$\min_{x \in X} \; c^T x$$
$$\text{s.t. } \inf_{\mathbb{P}_u \in U} \mathbb{P}_u \left(A(\tilde{\xi}) x \geq b(\tilde{\xi}) \right) \geq 1 - \epsilon \tag{5}$$

In DRCC, ϵ represents the worst-case probability of violating constraints $A(\tilde{\xi})x \geq b(\tilde{\xi})$ with respect to U.

C. Construction of the Ambiguity Set

In reality, the probability distribution $\mathbb{P}_u$ of a random variable ξ is not precisely known, and only limited historical data are available. However, constructing an ambiguity set U based on historical data can provide reasonable probabilistic information about $\mathbb{P}_u$. A properly constructed ambiguity set U should exhibit the following properties: 1) reflect the characteristics of the underlying true probability distribution, 2) be sufficiently small to allow for the integration of additional historical sample data, thereby reducing conservatism, and 3) ensure the tractability of the DRCC model. A good choice of ambiguity set U is an important element for the DRCC. This study implements the distance-based Wasserstein metric for the construction of the ambiguity set U, which is defined as a ball in the space of probability distribution. Given a series of N historical samples $\{\xi^s\}_{s=1}^{N}$ an empirical distribution is constructed as $\mathbb{P}_0(\tilde{\xi} = \xi^s) = \frac{1}{N}$ as an estimation of the reference distribution. The Wasserstein ambiguity set U in the space of probability distributions is given as:

$$U := \{\mathbb{P}_f \, \epsilon \, \mathcal{P} \; : W(\mathbb{P}_u, \mathbb{P}_0\} \leq \delta \tag{6}$$

where (6) represents a Wasserstein ball with a positive radius δ centered at an empirical distribution $\mathbb{P}_0$. The radius δ is an essential parameter in defining the ambiguity set U. It has direct control over the performance and degree of conservatism of the resulting decisions. The distance between $\mathbb{P}_u$ and $\mathbb{P}_0$ can be measured by using the Wasserstein metric.

$$W(\mathbb{P}_u, \mathbb{P}_0) := inf_{\mathbb{Q}\sim(\mathbb{P}_u,\mathbb{P}_0)} \mathbb{E}_{\mathbb{Q}} \left[\left\| \tilde{\xi}_1 - \tilde{\xi}_2 \right\|_p \right] \quad (7)$$

Here, $\tilde{\xi}_1$ and $\tilde{\xi}_2$ represents the random variable following the marginal probability distribution of $\mathbb{P}_u$ and $\mathbb{P}_0$ and $\mathbb{Q}\sim(\mathbb{P}_u, \mathbb{P}_0)$ denotes a joint distribution of $\tilde{\xi}_1$ and $\tilde{\xi}_2$. The expression $\|\cdot\|_p$ illustrate the p-norm where $p = 2$, and $\left\|\tilde{\xi}_1 - \tilde{\xi}_2\right\|_p$ represents the cost of moving a unit mass from $\tilde{\xi}_1$ to $\tilde{\xi}_2$.

D. *Mathematical Formulation of DRCC-LDM Model*

To mitigate the wildfire risk in the power system, while ensuring minimum load shedding, this paper proposes a DRCC-LDM model. Its objective function (8) minimizes the load shedding cost while satisfying the wildfire risk mitigation chance constraint (9).

$$\min_{x\in X, z\in Z, c\in C} \sum_{d\in D} c_d P_d^{LS} \quad (8)$$

where, $x \in X$ and $z \in Z$ denotes the binary decision variables which include the ON/OFF decisions for all transmission lines, and of generators and loads, respectively. In addition, $c \in C$ represents the continuous variable. Also, P_d^{LS} and c_d denotes the real power load shedding and its cost rate for the load *d*.

$$\inf_{\mathbb{P}_u \in U} \mathbb{P}_u \left(\sum_{j,k\epsilon L} \tilde{r}_{jk}^f \left(1 - x_{jk}^{on}\right) \geq \mu_{th}^f R_T^{MD} \right) \geq 1 - \epsilon \quad (9)$$

Here, $\tilde{r}_{jk}^f$ represents the wildfire risk associated with each transmission line jk, incorporating the influence of uncertain wind speed conditions on the ignition probability of the line. Constraint (9) ensures that the de-energization decisions ($x_{jk}^{on} = 0$) collectively reduce the wildfire risk by at least the level of $\mu_{th}^f R_T^{MD}$ where μ_{th}^f represents the user-defined threshold of wildfire risk reduction, and R_T^{MD} denotes the total maximum potential damage across all transmission lines' areas.

Constraint (9) is designed to manage wildfire risk within the power system through de-energization decisions, considering the impact of wind speed conditions on wildfire risk. It handles the left-hand side (LHS) uncertainty over the Wasserstein ambiguity set, where the probability of satisfying constraint (9) is allowed to be less than a specified risk tolerance ϵ.

The deterministic constraints of DRCC-LDM are below.

$$\sum_{d\in D} z_d^{on} P_d^D \geq \eta_{th} D_T \quad (10a)$$

$$P_d^{LS} = (1 - z_d^{on}) P_d^D \qquad \forall d \in D \quad (10b)$$

The expression in (10a) restricts the minimum proportion of system demand that needs to be satisfied, where z_d^{on} represents the proportion of the load, P_d^D is the real power demand of each load d, η_{th} is the percent/threshold limit, and D_T denotes the total demand of the system. The amount of load shedding for each load P_d^{LS} is defined in (10b).

$$P_{jk} \leq -b_{jk} \left(\theta_j - \theta_k + \theta^{max}\left(1 - x_{jk}^{on}\right)\right), \forall (j,k) \in L \quad (11a)$$

$$P_{jk} \geq -b_{jk} \left(\theta_j - \theta_k + \theta^{min}\left(1 - x_{jk}^{on}\right)\right), \forall (j,k) \in L \quad (11b)$$

Constraints (11a) and (11b) show the DC power flow where P_{jk} express the transmission line power flow, b_{jk} is the susceptance and θ_j and θ_k presents the voltage angle of the bus j and k. The introduction of big-M helps to reduce the model to a linearized DC power flow model, and θ^{max} and θ^{min} are the big-M values in (11a) and (11b).

$$-x_{jk}^{on} P_{jk}^{min} \leq P_{jk} \leq x_{jk}^{on} P_{jk}^{max}, \ \forall (j,k) \in L \quad (12)$$

Further, (12) enforces the capacity limit on the line flow by restricting the power flow of each line within its capacity limit, considering the ON/OFF status of the corresponding line.

$$\sum_{g\in B_j^G} P_g = \sum_{j,k\in B_j^L} P_{jk} + \sum_{d\in B_j^D} z_d^{on} P_d^D \quad \forall j \in B \quad (13)$$

The nodal power balance ensures that the total power generated in the system is enough to meet the load requirements in (13).

$$z_g^{on} P_g^{min} \leq P_g \leq z_g^{on} P_g^{max}, \qquad \forall g \in G \quad (14)$$

The upper and lower bounds of generators are given in (14).

III. Solution Methodology of DRCC-LDM Model

Due to the probabilistic nature of constraint (9), this section presents the methodology for solving the DRCC-LDM model. To handle the reformulation of constraint (9), assume $A(\tilde{\xi}) \neq 0$ for all $\tilde{\xi}$, and introduce auxiliary variables such as, $v \in \mathbb{R}, \gamma \in \mathbb{R}^N$, $y \in \{0,1\}^N$, and big-M constants s for $s = 1, \ldots, N$. Using these, the DRCC can be reformulated as a mixed-integer second-order conic problem (MISOCP).

This study adopts a conditional value-at-risk (CVaR) interpretation for the ambiguous chance constraint (9), where CVaR approximation of the DRCC can be expressed as:

$$Q = \frac{\delta}{\epsilon} + CVaR_{1-\epsilon} \left[-max \left\{ \left(\sum_{j,k\epsilon L} \tilde{r}_{jk}^f \left(1 - x_{jk}^{on}\right) \right) - \mu_{th}^f R_T^{MD}, 0 \right\} \right] \leq 0 \quad (15)$$

Also, our proposed DRCC-LDM problem formulates the Wasserstein distance (7) from each data sample $\tilde{r}_{jk,s}^f$ ($s = 1, \ldots, N$) to an unsafe set $\overline{S}(x)$ as,

$$W = \frac{max\left(\sum_{j,k\epsilon L} \tilde{r}_{jk,s}^f \left(1 - x_{jk}^{on}\right) - \mu_{th}^f R_T^{MD}, 0\right)}{\left\|\sum_{j,k\epsilon L} \left(1 - x_{jk}^{on}\right)\right\|_2} \quad (16)$$

Considering the CVaR and Wasserstein distance, and making the set Q mixed-integer representable, the Wasserstein ambiguity set U is constructed in the form (6) is feasible if and only if the following set of constraints is satisfied,

$$\epsilon v - \frac{1}{N} \sum_{s=1}^{N} \gamma_s \geq \delta \left\| \sum_{j,k\epsilon L} \left(1 - x_{jk}^{on}\right) \right\|_2 \quad (17)$$

$$max \left[\sum_{j,k\epsilon L} \tilde{r}_{jk,s}^f \left(1 - x_{jk}^{on}\right) - \mu_{th}^f R_T^{MD}, 0 \right] \geq -\gamma_s + v \quad (18)$$

Here, the maximum value of a term $\left(\sum_{j,k\epsilon L} \tilde{r}_{jk,s}^f \left(1 - x_{jk}^{on}\right) - \mu_{th}^f R_T^{MD}, 0\right)$, meaning that if the term is greater than zero, it returns the value of the term; otherwise, zero. The max operator in the constraint (19) makes it nonlinear and difficult to solve. The binary variable $y_s \in \{0,1\}$ and big-M constant M_s is introduced to linearize constraint (18), which always ensures the maximum value of $\left(\sum_{j,k\epsilon L} \tilde{r}_{jk,s}^f \left(1 - x_{jk}^{on}\right) - \mu_{th}^f R_T^{MD}, 0\right)$. So, the equivalent formulation of constraint (18) is as follows,

$$M_s(1 - y_s) \geq -\gamma_s + v, \ \forall s \quad (19)$$

$$\sum\nolimits_{j,k\epsilon L} \tilde{r}_{jk,s}^{f}\left(1-x_{jk}^{on}\right)-\mu_{th}^{f} R_{T}^{MD}+M_{s} y_{s} \geq -\gamma_{s}+v, \forall s \quad (20)$$

Moreover, the big-M constants M_s can be chosen by using coefficient strengthening techniques, such as

$$M_s = \left(\max_{x\in X, s=1,\ldots,N}\left\{\left(\sum\nolimits_{j,k\epsilon L} \tilde{r}_{jk,s}^{f}\left(1-x_{jk}^{on}\right)-\mu_{th}^{f} R_{T}^{MD}\right)\right\}\right)^{+} - \min_{x\in X}\left\{\left(\sum\nolimits_{j,k\epsilon L} \tilde{r}_{jk,s}^{f}\left(1-x_{jk}^{on}\right)-\mu_{th}^{f} R_{T}^{MD}\right)\right\}, \forall n \quad (21)$$

Here, the superscript "+" denotes the positive part, meaning that only positive values are considered, while negative values are set to zero. Finally, our DRCC-LDM with LHS uncertainty under the ambiguity set U leads to an MISOCP model which includes (8), (10), (11), (12), (13), (14), (17) and (19) – (21). And a solver, Gurobi v11.0, can be utilized to solve this model.

IV. Case Studies

This section uses the RTS-GMLC 73-bus test system [9] aimed at validating the performance of the proposed DRCC-LDM for wildfire risk mitigation. In this case study, to calculate the wildfire risk r_{jk}^{f}, we suppose a high-intensity fire ($I_{jk} = 3$) and maximum effect ($E_{jk} = 100\%$) in each line area. The load shedding cost c_d is set to \$1,000/MWh. The load supplied threshold limit η_{th} is assumed to be 30% of the original load, whereas the total demand in the system is 8,550 MW. The wildfire risk reduction threshold μ_{th}^{f} is set to 0.04. The value of risk tolerance ϵ and radius δ is set to 0.05 and 0.02. The following process is used to generate the wind speed scenarios over each transmission line area:

Step 1: Data Sampling: To capture the seasonal variations from the original dataset, two months' data were chosen from the annual data. One month depicts summer conditions, while the other month illustrates winter conditions. A total of 60-day data set is sorted and categorized into each period by using 24 hourly values of each day in order to prepare it for analysis. Step 2: Sample Generation: Using the sorted data, the parameters of the Weibull distribution - specifically the scale a and shape b parameters are estimated for each period by fitting the data to the Weibull distribution. Then, the inverse transform method is employed to obtain wind speed for each transmission line. Furthermore, a uniform distribution is applied to generate N wind speed samples for each transmission line.

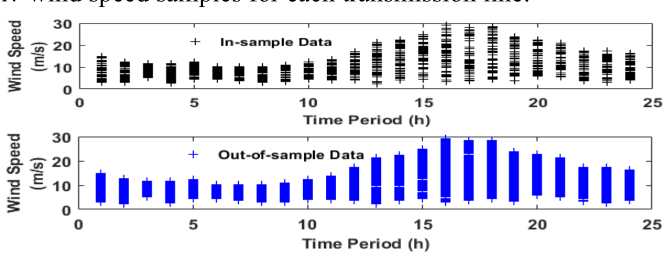

b)

Fig. 1. (a) 100 In-sample data, and (b) 300 out-of-sample data.

To obtain 24-hour wind speed samples, Step 2 is repeated for each time interval. For each line and period, 400 samples are generated, where 100 are randomly selected to construct the Wasserstein ambiguity set, and the remaining 300 are used for out-of-sample testing. Figure 1a shows the in-sample data for Line 1, while Figure 1b illustrates the out-of-sample data used for performance evaluation. The case study is conducted using wind speed data corresponding to period 17.

A. Comparison between Chance-Constrained Methods

This subsection provides a comparative analysis of typical CC and proposed DRCC models where the in-sample optimal solution is fixed at confidence levels (1-ϵ) of 90% and 95% to evaluate the out-of-sample performance. Table I presents the comparison of both methods in terms of the specified confidence levels, objective function, load delivered, average wildfire risk mitigation, and observed confidence level. As shown in Table I, at a 90% specified confidence level, CC has the lowest objective function cost of \$587,335 and delivers the highest load of about 7,962MW than DRCC. However, the average wildfire risk mitigation is lower, and the observed confidence level of CC in the out-of-sample analysis is about 88.7%, which is below the specified confidence level of 90%. DRCC results in the highest objective function cost of \$822,000 and supplies a smaller amount of load, which is 7,728MW. But DRCC achieves a higher average wildfire risk mitigation and a higher observed confidence level of about 96.4% than the CC.

TABLE I. Performance of Different Chance-Constrained Methods

Specified Confidence Level	Method	Objective Function (\$)	Load Delivered (MW)	Avg. Wildfire Risk Mitigation	Observed Confidence Level (%)
1-ϵ = 90%	CC	587,335	7962	8.87	88.7
	DRCC	822,000	7728	13.48	96.4
1-ϵ = 95%	CC	668,495	7881.5	9.31	92.0
	DRCC	997,000	7553	15.03	99.1

Also, both methods show a higher objective function cost and average wildfire risk mitigation at the 95% specified confidence level than at the 90%. In CC, the observed confidence level improves from 88% to 92%, but it is still below the specified confidence level of 95%. Similar to the 90% specified confidence level, DRCC performs better with the highest observed confidence level of 99%. Overall, DRCC provides a higher wildfire risk mitigation and observed confidence level.

B. Impact of Considering Uncertain Wind Speed Conditions

This subsection demonstrates the response of DRCC-LDM on line de-energization decisions based on the inclusion of the line characteristics and uncertain wind speed conditions. This case study compares three cases: Case 1 considers only line characteristics to estimate the probability of ignition, Case 2 considers only uncertain wind speed conditions for probability of ignition calculation, and Case 3 incorporates both. In Fig. 2, transmission lines are categorized as low, medium, or high-risk lines based on line characteristics. Also, the uncertain wind speed conditions range from 6 to 26 m/s, where low wind speeds correspond to 6–15 m/s, medium to 16 –21 m/s, and high to 22–26 m/s. In Case 1, when only line characteristics are considered, several medium and high-risk lines are de-energized because they have the possibility to initiate a fire, as shown in Fig. 2a. In Case 2, when only wind speed is considered, most lines experience wind speeds between 16 and 26 m/s, which substantially increases their probability of ignition. Consequently, the de-energized lines are those exposed to these medium-high wind speed conditions, as shown in Fig. 2b. In Case 3, when both line characteristics and uncertain wind speed conditions are considered, the lines exposed to wind speed from 16 to 26 m/s are de-energized because they exhibit a high probability of igniting fire.

979-8-3315-8138-1

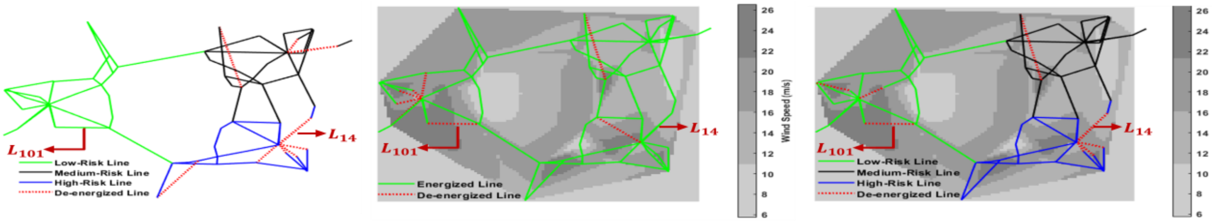

a) b) c)

Fig. 2. De-energization decisions of transmission lines based on wildfire risk estimated from a) Line characteristics, b) Uncertain wind speed, and c) Both.

Additionally, some high-risk lines due to line characteristics are also de-energized in Case 3. Comparing all cases, the line de-energization decisions depend on line characteristics and uncertain wind speed conditions to reduce wildfire risk. For example, line L_{101} is considered a low-risk line due to line characteristics and remains energized in Case 1 when only line characteristics are considered. However, L_{101} is de-energized in Cases 2 and 3 due to its exposure to wind conditions between 16 to 26 m/s, as shown in Fig. 2b and 2c. But L_{14} belongs to a high-risk line and is de-energized in Cases 1 and 3 due to its high probability of ignition based on the line characteristics, even though it experiences relatively low wind speeds of 11–15 m/s and remains energized in Case 2. Overall, the proposed model de-energizes lines that are at high risk of ignition based on the line characteristics and uncertain wind speed. The solution time to solve Case 3 is about 75 seconds.

C. *Impact of Varying Wasserstein Radius and Risk Tolerance*

This study explains the impact of varying Wasserstein radius δ on the load shedding as well as the varying impact of risk tolerance ϵ on both load shedding and average wildfire risk mitigation. Fig. 3a shows that when δ is small (0.01-0.03), the ambiguity set remains closer to reference distribution, resulting in less conservative solution with minimal load shedding. As δ increases, ambiguity set encompasses more possible distributions, the model becomes significantly more conservative, leading to increase in load shedding to nearly 50% of the total load. Moreover, in Fig. 3b, at lower values of ϵ, a higher confidence level enforces stricter requirement to constraint satisfaction, resulting in higher load shedding and higher average wildfire risk mitigation. As ϵ increases, the confidence level requirement is relaxed, that leads to lower load shedding and average wildfire risk mitigation.

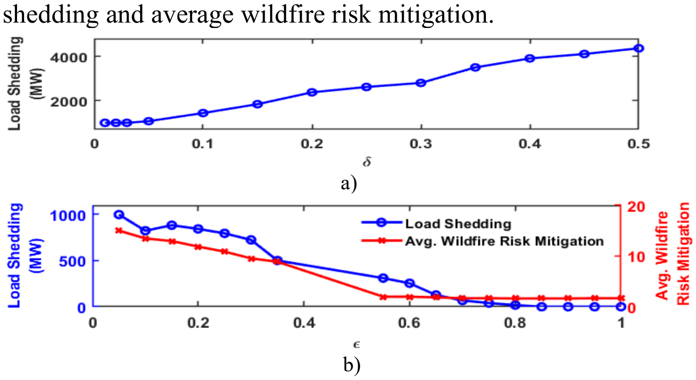

Fig. 3. Impact of varying (a) Wasserstein radius δ on the load shedding, and (b) risk tolerance ϵ on both load shedding and wildfire risk mitigation.

V. CONCLUSION

This paper proposes a wildfire-resilient operational strategy for power systems that mitigate wildfire risk under uncertain wind conditions. The approach integrates line characteristics and uncertain wind speed into the wildfire risk assessment and formulates the wildfire mitigation constraint as a chance constraint within the DRCC framework, ensuring system robustness under uncertainty. Case studies demonstrate that the proposed method achieves improved out-of-sample performance even with limited data information and provides lines de-energization decisions that account for uncertain wind speed conditions, highlighting its potential as an effective tool for proactive wildfire risk mitigation in power systems.

REFERENCES

[1] D. A. Z. Vazquez, F. Qiu, N. Fan, and K. Sharp, "Wildfire Mitigation Plans in Power Systems: A Literature Review," *IEEE Trans. on Power Syst,* vol. 37, no. 5, pp. 3540-3551, 2022.

[2] S. Jazebi, F. d. Leon and A. Nelson, "Review of Wildfire Management Techniques - Part I: Causes, Prevention, Detection, Suppression, and Data Analytics," *IEEE Trans. on Power Delivery,* vol. 35, no. 1, pp. 430-439, 2020.

[3] B. Sohrabi, A. Arabnya, M. P. Thompson, and A. Khodaei, "A Wildfire Progression Simulation and Risk-Rating Methodology for Power Grid Infrastructure," *IEEE Access,* 2024.

[4] Z CBC, "Texas wildfire likely caused by power line sparks," 2011. [Online]. Available: https://www.cbc.ca/news/world/texas-wildfire-ikely-caused-by-power-line-sparks-1.998388.

[5] W. F. C. Association, "The Link Between Power Lines and Wildfires," 2021. [Online]. Available: https://wfca.com/wildfire-articles/power-lines-and-wildfires.

[6] S. Jazebi, F. d. Leon and A. Nelson, "Review of Wildfire Management Techniques—Part II: Urgent Call for Investment in Research and Development of Preventative Solutions," *IEEE Trans. on Power Delivery,* vol. 35, no. 1, pp. 440-450, 2020.

[7] Pacific gas and electric company, "pacific gas and electric company amended 2019 wildfire safety plan," Tech. Rep., 2019.

[8] N. Rhodes, L. Ntaimo, and L. Roald, "Balancing wildfire risk and power outages through optimized power shut-offs," *IEEE Trans. Power Syst.,* vol. 36, no. 4, pp. 3118-3128, 2020.

[9] N. Rhodes, C. Coffrin, and L. Roald, "Security constrained optimal power shutoff for wildfire risk mitigation," *IET Generation, Transmission & Distribution,* vol. 18, no. 18, pp. 2972-2986, 2024.

[10] H. Yang, N. Rhodes, H. Yang, L. Roald, and L. Ntaimo, "Multiperiod Power System Risk Minimization under Wildfire Disruptions," *IEEE Trans. on Power Syst.*, vol. 39, no. 5, pp. 6305-6318, Jan. 2024.

[11] Y. Zhou, K. Sundar, H. Zhu, and D. Deka, "Mitigating the impact of uncertain wildfire risk on power grids through topology control," in *2024 18th International Conference on Probabilistic Methods Applied to Power Systems (PMAPS)*. IEEE, 2024, pp. 1–6.

[12] T. Tapia, Á. Lorca, D. Olivares, M. Negrete-Pincetic, and A. J. Lamadrid L, "A robust decision-support method based on optimization and simulation for wildfire resilience in highly renewable power systems," *Eur. J. Oper. Res*., vol. 294, pp. 723–733, Oct. 2021.

[13] J Z. Luo, Y. Yin, D. Wang, T. Cheng, and C.-C. Wu, "Wasserstein distributionally robust chance-constrained program with moment information," *Computers & Operations Research,* vol.152, 2023.

[14] S. R. Han, S. D. Guikema, S. M. Quiring, K. h. Lee, D. Rosowsky, and R. A. Davidson, "Estimating the spatial distribution of power outages during hurricanes in the Gulf Coast region," *Reliability Engineering & System Safety,* vol. 94, pp. 199-210, 2009.

979-8-3315-8138-1